Available online at www.sciencedirect.com
ScienceDirect
Surface & Coatings Technology 202 (2007) 1323–1328
SURFACE & COATINGS TECHNOLOGY
www.elsevier.com/locate/surfcoat

Performance of sol–gel deposited $Zn_{1-x}Mg_xO$ films used as active channel layer for thin-film transistors

Chien-Yie Tsay [a,*], Hua-Chi Cheng [b], Min-Chi Wang [a], Pee-Yew Lee [c], Chia-Fu Chen [b,d], Chung-Kwei Lin [a]

[a] Department Mater. Sci. Eng., Feng Chia University, Taichung, Taiwan
[b] Department Mater. Sci. Eng., National Chiao Tung University, Hsinchu, Taiwan
[c] Inst. Mater. Eng., National Taiwan Ocean University, Keelung, Taiwan
[d] Inst. Mater. Eng., Ming Dao University, Changhua, Taiwan

Available online 11 August 2007

Abstract

ZnO thin-film transistors (TFTs) have attracted considerable R&D interest due to their high transparency and low photosensitivity compared with typical a-Si:H TFTs. The electrical characteristics of ZnO thin films may be controlled by doping with ternary element, for instance Al, Ga, In, Mg, Zr, etc. In this study, $Zn_{1-x}Mg_xO$ ($x=0$ to 0.36) thin films were deposited on glass substrates by spin coating. The as-deposited films were baked at 300 °C for 10 min and then annealed at 500 °C for 1 h in air. The results show that, addition of Mg-species in ZnO films markedly enhanced the uniformity of film thickness and improved optical properties. The $Zn_{0.8}Mg_{0.2}O$ film exhibited the best transparency of 92%, an increase of ~15% over a pure ZnO film, and the rms roughness value decreased to 1.63. The $Zn_{1-x}Mg_xO$ TFTs were demonstrated to have n-type enhancement behavior. The optimum device with $Zn_{0.8}Mg_{0.2}O$ channel layer had a field-effect mobility of 0.1 cm^2/V s, a threshold voltage of 6.0 V, and an on/off ratio more than 10^7.

Keywords: $Zn_{1-x}Mg_xO$ films; Sol–gel method; Thin-film transistors

1. Introduction

Zinc oxide (ZnO) is an n-type II–VI group compound semiconductor material with direct wide bandgap of 3.35 eV. Due to its unique electrical and optical properties it has been widely and popularly used in varistor, gas sensor, UV light emitters and surface acoustic wave devices [1]. Recently, ZnO films also attracted attention for energy and optical–electrical applications, such as window layers of solar cells [2], transparent conductive layers of flat panel displays or touch panels [3] and the active channel layer of thin-film transistors [4]. The TFTs array fabrication process for large-area TFT-LCD has been continuously developed for simple processing steps, improving performance and reducing cost in the process of mass production. The sol–gel method offers a simple and low cost thin-film deposition process as an alternative to the vacuum deposition technique, but it needs soluble types of materials. The carrier mobility of the intrinsic ZnO materials exceed the field-effect mobility of a-Si:H which is the active channel layer in a typical TFT array. ZnO base TFTs possess low photosensitivity and high transparency, and have been studied by many groups [4–7], but only a few reported using chemical solution processes for ZnO film deposition. Norrs et al. [8] reported fabrication of an un-doped ZnO TFT using spin coating. Lee et al. prepared $Zn_{1-x}Mg_xO$ thin films [9] and $Zn_{1-x}Zr_xO$ thin films [10] as active channel using dip coating and spin coating, respectively. Besides, Cheng et al. [11] also fabricated the transparent ZnO TFT using a combined method of the sol–gel and chemical bath deposition.

It has been demonstrated that the electrical characteristic of ZnO thin films could be controlled by doping with ternary element, for instance Al, Ga, In, Mg, Zr, etc. The incorporation of Mg into ZnO tends to decrease the amount of interstitial oxygen vacancies [12]. Moreover, the study of Lee et al. [9] have illustrated that the depletion region in the grains increased

* Corresponding author. Fax: +886 4 24510014.
E-mail address: cytsay@fcu.edu.tw (C.-Y. Tsay).

0257-8972/$ - see front matter © 2007 Elsevier B.V. All rights reserved.
doi:10.1016/j.surfcoat.2007.07.080

with amount of Mg doping and resulted the almost depleted grains in the active layer of $Zn_{1-x}Mg_xO$ TFT. The ionic radii of Mg^{+2} (0.65 Å) and Zn^{+2} (0.74 Å) are similar, and thus the limit of solid solubility of MgO in ZnO can approach 40 at.% [13,14]. Many reports show that the solubility limit of Mg content in $Zn_{1-x}Mg_xO$ films strongly depend on deposition or growth technique, e.g. MOVPE [14], PLD [13,15], sputter [16] and sol–gel method [17,18].

In the present study, dense ZnO thin films with or without doping with Mg^{+2} were prepared using the sol–gel method and microstructure, optical properties affected by Mg content were investigated. Moreover, $Zn_{1-x}Mg_xO$ channel TFTs were fabricated and electrical characteristics of optimum devices evaluated.

2. Experimental

Zinc acetate dehydrate ($Zn(CH_3COO)_2{\cdot}2H_2O$) and magnesium acetate tetra-hydrate ($Mg(CH_3COO)_2{\cdot}4H_2O$) were dissolved in 2-methoxyethanol, and then monoethanolamine (MEA) was added to the solution. The concentration of metal ions in $Zn_{1-x}Mg_xO$ sols were controlled at 0.75 M and Mg^{+2} was varied from 0 to 0.36 (for x values). The solution was stirred for 2 h at 60 °C until a clear and homogenous sol was obtained. The $Zn_{1-x}Mg_xO$ thin film was deposited on alkali-free glass (Corning 1737) using the spin coating method, using 3000 rpm for 20 s. These as-coated films were baked at 300 °C for 10 min, and then annealed at 500 °C for 1 h in air.

Thermal analysis of the $Zn_{1-x}Mg_xO$ sols used TG-DSC (TA Instrument, SDT 2960) to identify the evaporation, decomposition and crystallization points of the $Zn_{1-x}Mg_xO$ solution material. The crystal structure and microstructure of these thin films were examined using X-ray diffractometry (XRD, MAC Science MAXP3) and scanning electron microscopy (SEM, HITACHI S-4800), respectively. Surface morphology of the $Zn_{1-x}Mg_xO$ thin films was observed by scanning probe microscope (SPM, Digital Instrument NS4/D3100CL). Optical transmittance spectra in the visible range of these films were examined by a spectrophotometer (Mini-D2T, Ocean Optics Inc.).

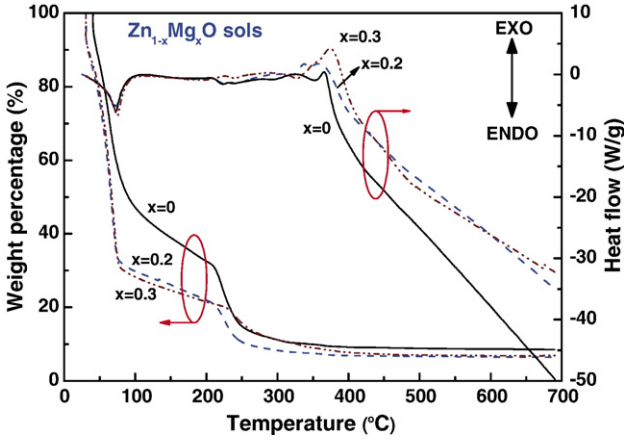

Fig. 1. TGA-DSC curves of the dried of $Zn_{1-x}Mg_xO$ sols with x=0, 0.2 or 0.3.

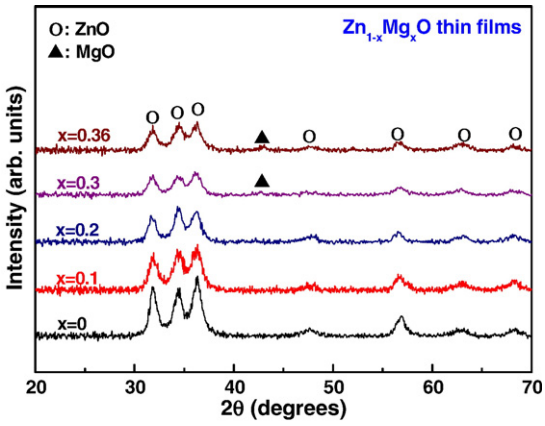

Fig. 2. X-ray diffraction patterns of $Zn_{1-x}Mg_xO$ thin films ($0 \leqq x \leqq 0.36$), which were annealed at 500 °C for 1 h.

The typical bottom-gate structure device of $Zn_{1-x}Mg_xO$ TFTs was fabricated by a hybrid method that combined the standard micro-electrical fabricated process and sol–gel method. The MoW film (1000 Å thick) was deposited and patterned on a glass substrate as a bottom-gate electrode. Silicon dioxide, prepared by plasma enhanced chemical vapor deposition (PECVD), served as the gate insulator with thickness 3000 Å. The source and drain select ITO thin-film patterns were defined by standard photolithography process. The channel length and width of the test device were 500 and 60 μm, respectively. Finally, the active layer, $Zn_{1-x}Mg_xO$ thin film, was deposited by the spin coating method to finish the $Zn_{1-x}Mg_xO$ TFTs. The current–voltage (I–V) characteristics of the transistors with $Zn_{1-x}Mg_xO$ channel layer were performed by semiconductor parameter analyzer (HP 4155B). Grain boundaries of polycrystalline ZnO films generally contain a wide distribution of deep-level traps [19]. This factor can affect the donor density of active layer and mobility of the TFT. In order to minimize this effect, voltage sweep ranged from −100 to 100 V or 0 to 100 V was performed prior to the I–V measurements.

3. Results and discussion

Thermogravimetric analysis (TGA) and differential scanning calorimetry (DSC) of pure ZnO, $Zn_{0.8}Mg_{0.2}O$ and $Zn_{0.7}Mg_{0.3}O$ sols are shown in Fig. 1. In TGA curves of dried un-doped ZnO and $Zn_{1-x}Mg_xO$ precursors, weight losses were observed with three temperature regions at 40 ~ 90, 100 ~ 200 and 210 ~ 260 °C. The first weight loss region is caused by low temperature solvent evaporation. The second and third weight loss regions are due to evaporation of water and decomposition of organic compounds. The raw source material for the Mg ions, magnesium acetate tetra-hydrate, possesses double the water of crystallization than zinc acetate. For this reason, there are lower solid content in the Mg-doped ZnO sols. Moreover, one large and two small endothermic peaks, and an exothermic peak were found in DSC curves of dried un-doped and Mg-doped ZnO sols. The last peak of the DSC curve, the exothermic peak, results from the crystallization of $Zn_{1-x}Mg_xO$ materials. It may be noted that, the effect of

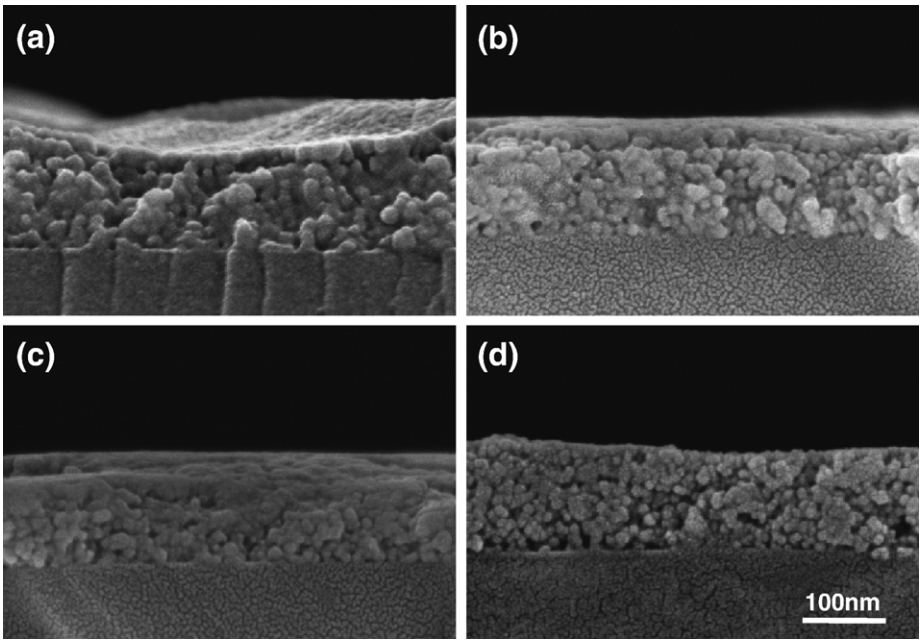

Fig. 3. SEM micrographs of cross-sections of $Zn_{1-x}Mg_xO$ thin films: (a) $x=0$; (b) $x=0.2$; (c) $x=0.3$ and (d) $x=0.36$.

Mg-doped ZnO can raise and broad this exothermic peak. It reveals the prepared of $Zn_{1-x}Mg_xO$ thin films can tolerate a wider process window.

All the $Zn_{1-x}Mg_xO$ ($x=0\sim0.36$) thin films were baked at 300 °C for 10 min and then annealed at 500 °C for 1 h in air. The crystallographic structure of thin films was studied by X-ray diffraction. Fig. 2 shows the XRD patterns of these $Zn_{1-x}Mg_xO$ thin films, which observed that they had wurzite structure. Crystallized ZnO has a hexagonal crystal structure which was confirmed by the three main diffracted peaks for the (100), (002) and (101) planes. The diffractograph also shows that the intensity of these main peaks reduce with increasing Mg content and the $Zn_{0.8}Mg_{0.2}O$ film shows a highly *c*-axis oriented (002) peak. Besides, a significant shift in the (002) and (001) peaks is observed after Mg doping. Dhananjay and Krupanidhi [16] have reported, Mg^{+2} replaced Zn^{+2} can increase the *a*-axis length and decrease *c*-axis of unit cells, and this transformation may have caused the two main peaks to shift. In the XRD patterns of $Zn_{0.7}Mg_{0.3}O$ and $Zn_{0.64}Mg_{0.36}O$ films, the diffracted peak of the MgO cubic phase was found at 42.9 degrees theta which is its (200) plane. The results show that at a Mg content more than 30 at.% the MgO phase became segregated. An MgO phase separate from the $Zn_{1-x}Mg_xO$ film can cause degeneration of electrical and optical properties. In previously

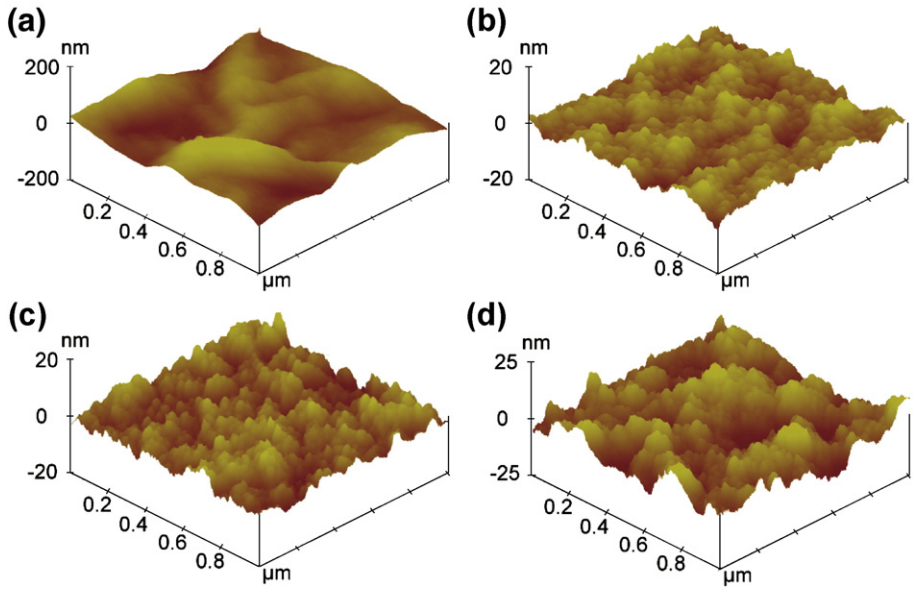

Fig. 4. SPM images of the surface of $Zn_{1-x}Mg_xO$ thin films: (a) $x=0$; (b) $x=0.2$; (c) $x=0.3$ and (d) $x=0.36$.

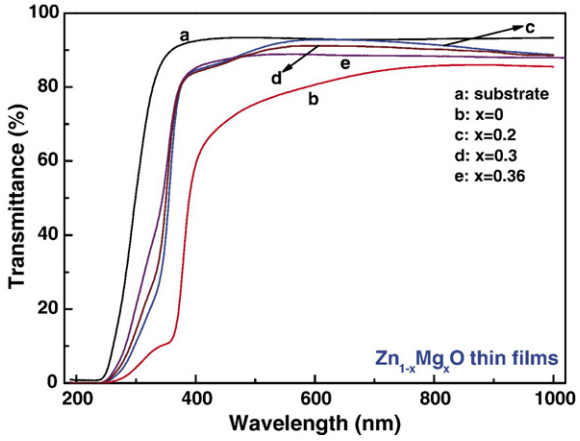

Fig. 5. The transmittance spectra of $Zn_{1-x}Mg_xO$ thin films with $x=0$, 0.2, 0.3 or 0.36.

mentioned research, many reports show that the solubility limit of Mg in $Zn_{1-x}Mg_xO$ films strongly depends on deposition or growth technique. Thus, in order to retain the $Zn_{1-x}Mg_xO$ film's pure hexagonal crystal structure, the content of Mg^{+2} should not be more than $x=0.3$ according to our research.

The sol–gel method is a simple oxide thin-film deposition technique. It is possible to control the film thickness by merely adjusting the solution viscosity or coating times. On the top view SEM image of annealed pure ZnO film can observe which surface overspread abnormally erumpent streak (not shown). However, these doped samples cannot observe that appearance. Cross-sectional SEM images of the $Zn_{1-x}Mg_xO$ thin films are shown in Fig. 3. Fig. 3(a) is an SEM micrograph of the ZnO film that shows its average thickness is about 140 nm. SEM micrographs of the nanocrystalline $Zn_{1-x}Mg_xO$ films ($x=0.2$, 0.3 and

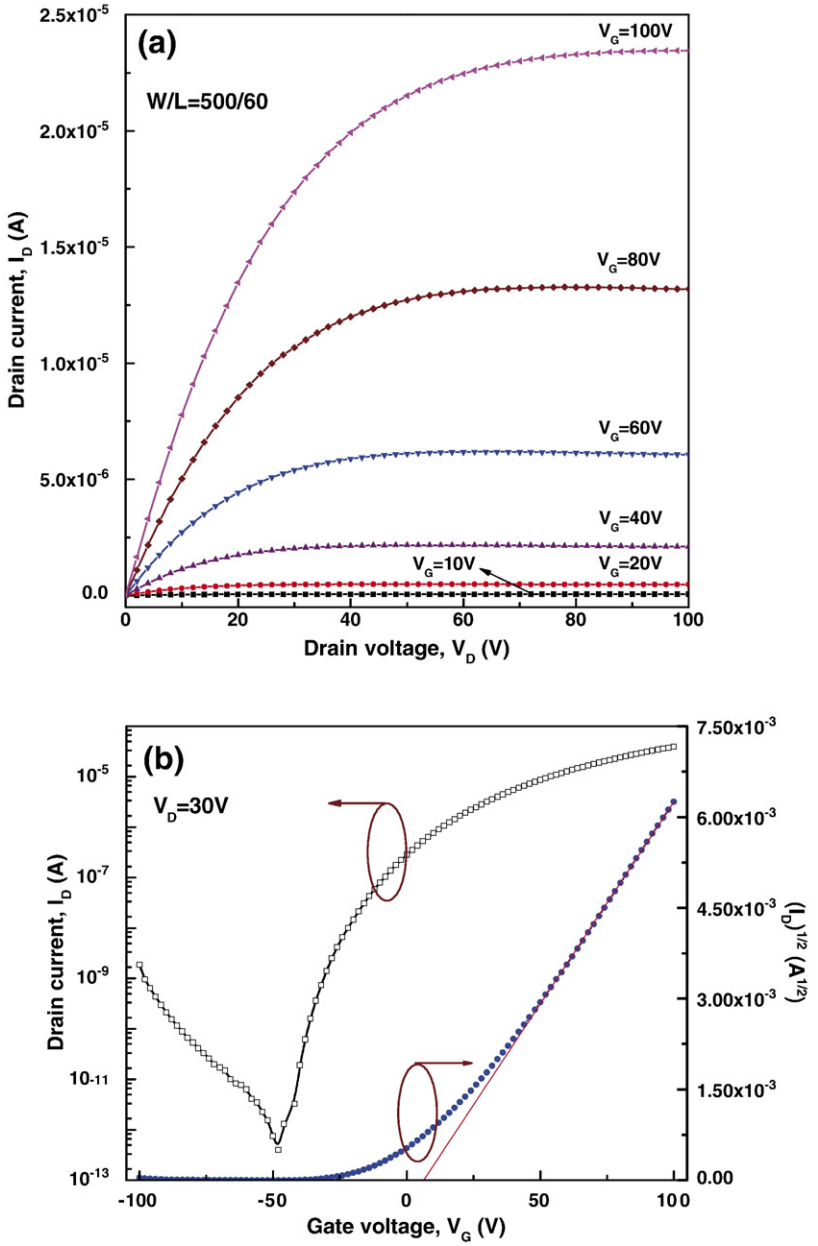

Fig. 6. (a) Output characteristics (I_D–V_D curve) and (b) transfer characteristics (I_D–V_G curve) of TFT using $Zn_{0.8}Mg_{0.2}O$ thin film as the active channel layer.

0.36) are shown in Fig. 3(b)–(d). They show that the thickness of doped film is about 150 nm. They also show that addition of Mg-species to the ZnO films markedly enhanced the uniformity of film thickness. The average grain sizes of the pure ZnO and Mg-doped films were about 20 nm and 10 ~ 15 nm, respective. These SEM images (Fig. 3) reveal that Mg doping of ZnO films can reduce the average grain size and improve the flatness of the $Zn_{1-x}Mg_x$ films. In addition, micrography of the $Zn_{0.64}Mg_{0.36}O$ film, show in Fig. 3(d) revealed a porous and non-compact microstructure. It exhibit poorer film quality with x value than over 0.3. SPM images of the $Zn_{1-x}Mg_xO$ thin films are shown in Fig. 4. The surface morphology observed shows the influence of the Mg doping on the ZnO thin film. It is apparent that reduction of surface roughness results from the decrease in average grain size in ZnO film after Mg doping. The rms roughness of the ZnO and $Zn_{0.8}Mg_{0.2}O$ thin films was 16.24 and 1.63 nm, respectively. A significant improvement of surface roughness with Mg doping can be noticed. In addition, $Zn_{0.8}Mg_{0.2}O$ thin film also exhibited the smallest rms roughness among all of the annealed $Zn_{1-x}Mg_xO$ thin films investigated in the present study. The phase segregated impurities of $x=0.3$ and $x=0.36$ samples degenerated the surface texture of the thin films, and their rms values were 1.97 and 3.61, respectively.

Fig. 5 shows the optical properties of the $Zn_{1-x}Mg_xO$ thin films when examined at room temperature. From this figure, all samples showed sharp absorption edges in the UV region and this absorption edge shifted to shorter wavelengths when ZnO thin film was doped with Mg. The optical transmittance in the visible range for the pure ZnO film was about 80% and exhibited absorption edge at about 362 nm (curve b in Fig. 5). The Mg-doped samples show higher transparency compared with the un-doped sample. However, the transmittance spectra of higher Mg content samples, when $x \geqq 0.3$, showed a slight decrease in the 500 to 800 nm region. This result is in good agreement with the results of XRD, SEM and SPM and relates to Mg phase segregation. In this study, the $Zn_{0.8}Mg_{0.2}O$ sample exhibited the best transparency among doped samples of 92%, which represents an increase of about 15% over the un-doped ZnO sample.

The electrical characteristics of the devices show that all $Zn_{1-x}Mg_xO$ TFTs operated in n-type enhancement mode due to require a positive gate voltage to turn it on. A polycrystalline semiconductor thin film with single phase, defect free and uniform thickness can provide the fine channel layer for carrier propagation from source to drain [20]. The $Zn_{0.8}Mg_{0.2}O$ TFTs were optimum devices that displayed the best performance in the study. This result is in good agreement with the previous discussions of the current study. Fig. 6(a) shows the representative output characteristics (drain current–drain voltage, I_D–V_D) of the $Zn_{0.8}Mg_{0.2}O$ TFT measured at room temperature. The slope of each I_D curve is flat for large V_D, and hard saturation was observed. Fig. 6(b) shows the corresponding transfer characteristics (I_D–V_G) of the same device, measured at a fixed V_D of 30 V. This I_D–V_G curve reveals a drain current on to off ratio of more than 10^7. The threshold voltage (V_{th}) was defined by fitting a straight line and then intercepting the x-axis of the $(I_D)^{1/2}$–V_G plot. At the same time, the field-effect mobility (μ_{sat}) was determined by the following square equation [21]:

$$I_{D(sat)} = \mu_{sat} C_{OX} \left(\frac{W}{2L}\right)(V_G - V_{th})^2, \text{for } V_D \ll (V_G - V_{th})$$

where W is the channel width, L is the channel length, C_{OX} is the unit capacitance of gate insulator, V_{th} is the threshold voltage and μ_{sat} is mobility in the saturated current region. The V_{th} and μ_{sat} of the $Zn_{0.8}Mg_{0.2}O$ TFT were calculated to be 6.0 V and 0.1 $cm^2\ V^{-1}\ s^{-1}$, respectively.

4. Conclusions

Preparation and characterization of thin-film transistors with Mg-doped ZnO films for the active channel layer were investigated. The results show that Mg^{+2} doped ZnO films of the form $Zn_{1-x}Mg_xO$ had markedly improved surface texture (reduced roughness), optical properties and finer microstructure than ZnO films. The $Zn_{0.8}Mg_{0.2}O$ film exhibited the best transparency at 92%, increasing by 15% value for the un-doped ZnO film (80%), and its rms roughness value decreased to 1.63. When the Mg content exceeded 0.3 (× value) MgO phase segregation would occur. This impurity phase caused the film quality to degenerate. In this study, the $Zn_{1-x}Mg_xO$ TFTs were fabricated using the sol–gel method and exhibited n-type enhancement mode. The optimum device with $Zn_{0.8}Mg_{0.2}O$ channel layer has a field-effect mobility of 0.1 cm^2/V s, a threshold voltage of 6.0 V, and an on/off ratio more than 10^7.

Acknowledgments

The authors gratefully acknowledge the financial support by the National Science Council of Republic of China under contract no. NSC 95-2221-E-035-006 and Taiwan TFT-LCD Association (TTLA) under contract no. A643TT1000-S11.

References

[1] S.J. Pearton, D.P. Norton, K. Ip, W.W. Heo, J. Vac. Sci. Technol., B 22 (2004) 932.
[2] C.S. Ferekides, R. Mamazza, U. Balasubramanian, D.L. Morel, Thin Solid Films 480–481 (2005) 224.
[3] T. Minami, T. Miyata, Y. Ohtani, Y. Mochizuki, Jpn. J. Appl. Phys. 45 (2006) L409.
[4] R.L. Hoffman, J. Appl. Phys. 95 (2004) 5813.
[5] E. Fortunato, P. Barquinha, A. Pimentel, A. Gonçalves, A. Marques, L. Pereira, R. Martins, Thin Solid Films 487 (2005) 205.
[6] C.J. Kao, Y.W. Kwon, Y.W. Heo, D.P. Norton, S.J. Pearton, F. Ren, G.C. Chi, J. Vac. Sci. Technol., B 23 (2005) 1024.
[7] S. Masuda, K. Kitamura, Y. Okumura, S. Miyatake, J. Appl. Phys. 93 (2003) 1624.
[8] B.J. Norris, J. Anderson, J.F. Wager, D.A. Keszler, J. Phys. D: Appl. Phys. 36 (2003) L105.
[9] J.H. Lee, P. Lin, C.C. Lee, J.C. Ho, Y.W. Wang, Jpn. J. Appl. Phys. 44 (2005) 4784.
[10] J.H. Lee, P. Lin, J.C. Ho, C.C. Lee, Electrochem. Solid-State Lett. 9 (2006) G117.
[11] H.C. Cheng, C.F. Chen, C.Y. Tsay, Appl. Phys. Lett. 90 (2007) 012113.
[12] Y. Ogawa, S. Fujihara, Phys. Status Solidi (a) 202 (2005) 1825.

[13] J.W. Kim, H.S. Kang, J.H. Kim, S.Y. Lee, J.K. Lee, M. Nastasi, J. Appl. Phys. 100 (2006) 033701.
[14] W.I. Park, G.C. Yi, H.M. Jang, Appl. Phys. Lett. 79 (2001) 2022.
[15] T. Maemoto, N. Ichiba, S. Sasa, M. Inoue, Thin Solid Films 486 (2005) 174.
[16] Dhananjay, S.B. Krupanidhi, Appl. Phys. Lett. 89 (2006) 082905.
[17] C.S. Suchand Sandeep, R. Philip, R. Satheeshkumar, V. Kumar, Appl. Phys. Lett. 89 (2006) 063102.
[18] D. Zhao, Y. Liu, D. Shen, Y. Lu, J. Zhang, X. Fan, J. Cryst. Growth 234 (2002) 427.
[19] F.M. Hossain, J. Nishii, S. Takagi, A. Ohtomo, T. Fukumura, H. Fujioka, H. Ohno, H. Koinuma, M. Kawasaki, J. Appl. Phys. 94 (2003) 7768.
[20] Y. Kwon, Y. Li, Y.W. Heo, M. Jones, P.H. Hollyway, D.P. Norton, Z.V. Park, S. Li, Appl. Phys. Lett. 84 (2004) 2685.
[21] T. Tsukada, TFT/LCD: Liquid-Crystal Displays Addressed by Thin-Film Transistors, Gordon and Breach Publishers, Tokyo, 1996, p. 59.